CONTAMINATED SEDIMENT CAPPING: PROPWASH MODELING AND APPLICATION

V. Shepsis, PhD, P.E.[1], S. Fenical, P.E.[2], M. Tirindelli[3]

ABSTRACT

New generations of propwash computer models have been developed under a U.S. Federal Government grant from the Civilian Research and Defense Foundation (CRDF) to address dredging and coastal industry needs in designing contaminated sediments, caps and protections of natural habitats. The computer models have been used on feasibility, environmental impact and design studies for various projects in Washington, Texas, Louisiana and California. The paper discusses the development, implementation and verification of the advanced computer modeling tools, as well as constructed projects that were designed with the assistance of the new tools.

Keywords: Cap Design, Scour Protection, Numerical Modeling, Jet Hydrodynamics and Propeller Hydrodynamics

INTRODUCTION

Contaminated Sediment Capping (CSC) projects are typically located in open waters that are subjected to propeller wash effects of passing deep draft vessels, tugs, and small craft. Evaluating the propeller induced hydrodynamic forces on surface sediment and the sediment cap is critical to the CSC project design. Therefore, a state-of-the-art numerical modeling of propeller wash effects has become an essential part of the design procedure to provide reliable engineering recommendations with regard to the type and size of cap material, thickness of capping layer, spatial alignment, durability, etc.

PREVIOUS MODELING APPROACHES

Typical approaches to propwash modeling consisted of 1-dimensional or 2-dimensional steady-state analytical models developed by Albertson et al. (1948) and further modified by Blaauw (1978), Verhey (1983), Fuerher et al. (1987), Maynord (2000), Shepsis et al. (2000), and others. These models are based on semi-empirical formulation of the velocity field generated by jets discharging into a fluid body and by propellers rotating in a fluid. Formulas describe the velocities and geometry of the turbulent jet as it expands into a volume of water. The structure of the water velocity is described mathematically in two zones (Figure 1).

[1] Principal, Coast & Harbor Engineering, Inc., 110 Main Street, Suite 103, Edmonds, WA 98020, Phone (425) 778-6733, Fax (425) 778-6883, email: vladimir@coastharboreng.com

[2] Principal, Coast & Harbor Engineering, Inc., 388 Market Street, Suite 500, San Francisco, CA 94111, Phone (415) 296-3822, Fax (415) 276-3784, email: scott@coastharboreng.com

[3] Coastal Engineer, Coast & Harbor Engineering, Inc., 388 Market Street, Suite 500, San Francisco, CA 94111, Phone (415) 296-3842, Fax (415) 520-0107, email: matteo@coastharboreng.com

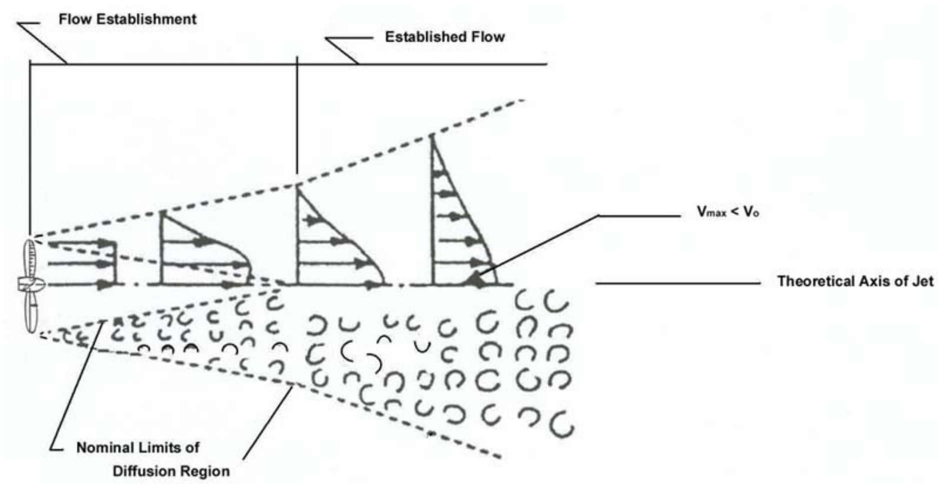

Figure 1. Geometry of initial velocity zone and momentum jet formed by propulsion system.

The VH-PS model (Vessel Hydrodynamics - Propwash Steady) has been developed and successfully used for various projects in the U.S. and overseas for several years. The VH-PS model is a steady-state, semi-analytical/semi-empirical model that solves equations for initial velocities generated by a propeller and velocity at given positions away from the propeller based on the momentum jet theory. The VH-PS model includes various algorithms, such as the equation for initial velocity (Equation 1), jet centerline velocity (Equation 2) and velocity pattern in the momentum jet (Equation 3):

$$V_0 = 1.6 \cdot n \cdot D_p \cdot \sqrt{K_{t_p}} \tag{1}$$

$$V_{MAX} = V_O \cdot \left(\frac{2 \cdot C \cdot X}{D_O} \right)^{-b} \tag{2}$$

$$V(x,r) = V_{MAX} \cdot \exp\left(-\frac{r^2}{2 \cdot X^2 \cdot C^2} \right)^{-b} \tag{3}$$

Where:

N = propeller rotation rate (revolutions per sec)

D_p = propeller diameter in meters

K_{t_p} = the thrust coefficient specific to the propeller [non-ducted propeller]

ρ = density of water

C, b = empirical constants (Verhey recommends *C* = 0.18 and *b* = 1.0)

D_0 = the effective propeller diameter

r = the radial distance from the jet centerline

The height above the bottom can be determined at any *X* in terms of the *r* magnitude. VH-PS allows user input of the height above bottom at which velocity is to be calculated. Therefore velocity measured at any known height can be compared with modeled velocity by correctly specifying the reference height variable. The VH-PS model was calibrated using propeller wash velocity field measurements collected in 1996, 1999, and 2000 at various locations in Puget Sound (Shepsis et al. 2000). The results of the comparison of the computer modeling (calibrated model) with field data are shown in Figure 2. The calibrated VH-PS model has been used successfully for various projects in Puget Sound and in other areas.

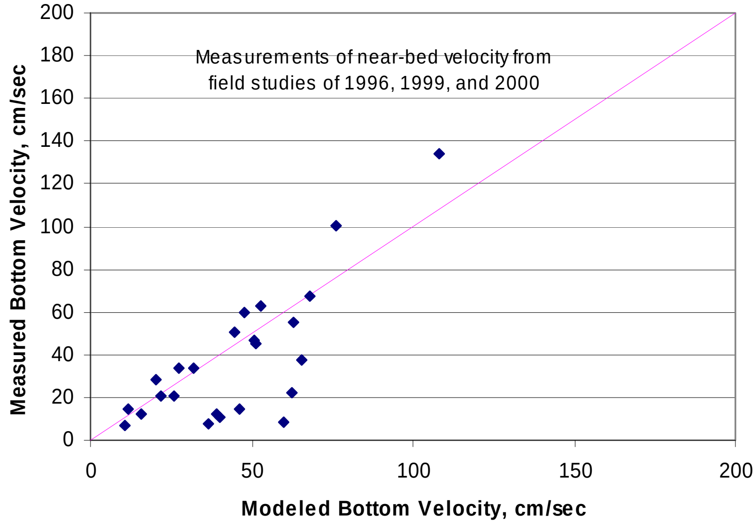

Figure 2. Comparison of VH-PS model predicted and measured propeller wash bottom velocities.

NEW MODELING APPROACHES

A new propwash modeling approach and numerical modeling tools was developed under a U.S. Civilian Research and Development Foundation grant and has been successfully used to enhance the abilities of design engineers and ultimately make CSC projects more economical and less susceptible to the risk of failure. The new propwash numerical model VH-PU (Vessel Hydrodynamics – Propwash Unsteady) is a 3-dimensional unsteady time-domain numerical model, based on solving for time-varying 3-dimensional velocity fields generated by ship propellers and jets in a curvilinear domain of arbitrary depth, spatial configuration while using a sigma vertical coordinate system. The model was developed with its base as a non-hydrostatic extension of the Princeton Ocean Model (POM) described by Blumberg and Mellor (1987), and was described in Kanarska and Maderich (2003).

In the model the 3D Reynolds averaged Navier-Stokes equations are used:

$$\frac{\partial u_i}{\partial xi} = 0, \tag{4}$$

$$\frac{\partial u_i}{\partial t} + u_j \frac{\partial u_i}{\partial x_j} = -\frac{1}{\rho_0}\frac{\partial p}{\partial x_j} - \frac{\partial \overline{u_i u_j}}{\partial x_j} - g_j, \tag{5}$$

where: $x_i = (x, y, z)$ are spatial coordinates, axis z is directed upward, $u_j = (u, v, w)$ are components of velocity, p is pressure, $g_j = (0, 0, g)$ is gravity, ρ_0 is constant density in Boussinesq approximation. The Reynolds stresses are modeled using the eddy viscosity approach:

$$\overline{u_i u_j} = -K_M\left(\frac{\partial u_i}{\partial x_j} + \frac{\partial u_j}{\partial x_i}\right) + \frac{1}{3}q^2\delta_{ij}, \tag{6}$$

where the eddy viscosity coefficient:

$$K_M = S_M ql \tag{7}$$

is related to the kinetic energy of turbulence:

$$\frac{1}{2}q^2 = \overline{u_i u_i} \tag{8}$$

and length scale l. Here S_M is a model constant. The model of turbulence is q-$q^2 l$, which is a 3-D extension of the model of Mellor and Yamada (1982):

$$\frac{\partial q^2}{\partial t} + u_j\frac{\partial q^2}{\partial x_j} = -2\overline{u_i u_j}\frac{\partial u_j}{\partial x_j} + \frac{\partial}{\partial x_j}S_q ql\frac{\partial q^2}{\partial x_j} - 2\frac{q^3}{B_1 l}, \tag{9}$$

$$\frac{\partial q^2 l}{\partial t} + u_j\frac{\partial q^2 l}{\partial x_j} = -E_1 l\overline{u_i u_j}\frac{\partial u_j}{\partial x_j} + \frac{\partial}{\partial x_j}S_l lq\frac{\partial q^2}{\partial x_j} - \frac{q^3}{B_1}\left[1 + E_2\left(\frac{1}{\kappa L}\right)\right], \tag{10}$$

In equation (2.5) the last term in square brackets is the wall function, which is necessary in a q-$q^2 l$ model to correctly describe flow near the solid boundary. Accordingly to Mellor and Yamada (1982), the distance from solid boundary L is:

$$L^{-1}(\mathbf{r}) = \frac{1}{2\pi}\iint\frac{dA(\mathbf{r}_0)}{[\mathbf{r} - \mathbf{r_0}]^3}, \tag{11}$$

Where: $\mathbf{r}$ is the radius vector for a given point, $\mathbf{r_0}$ is solid boundary. When the scale of computational domain is mainly a horizontal scale, then approximately:

$$L^{-1} = z^{-1} + (H - z)^{-1} \tag{12}$$

The constants of the turbulence model S_M, B_1, E_1, E_2 and S_l were determined by Mellor and Yamada (1982).

Boundary Conditions

The kinematic boundary condition at the water surface $z = \eta(x,y,t)$ is:

$$\frac{\partial\eta}{\partial t} + u\frac{\partial\eta}{\partial x} + v\frac{\partial\eta}{\partial y} = w \tag{13}$$

The dynamic condition is:

$$k_m \frac{\partial \mathbf{V_h}}{\partial z} = \frac{\boldsymbol{\tau_0}}{\rho_o} \tag{14}$$

where $\mathbf{V_h} = (u,v)$, $\boldsymbol{\tau} = (\tau^{(x)}, \tau^{(y)})$ is wind stress. At the nearest computational layer $z = H + z_b$,

$$-u\frac{\partial H}{\partial x} - v\frac{\partial H}{\partial y} = w \tag{15}$$

and

$$k_m \frac{\partial \mathbf{V}_h}{\partial z} = \frac{\boldsymbol{\tau}_b}{\rho_o}, \tag{16}$$

where:

$$\boldsymbol{\tau_b} = \rho_0 C_D \left|\mathbf{V_b}\right| \mathbf{V_b}, \tag{17}$$

$$C_D = \max\left(0.0025; \left(\frac{1}{\kappa}\ln(\frac{z_b + z_o}{z_o})\right)^{-2}\right) \tag{18}$$

The relevant boundary conditions for Equations 7 - 9 at the surface and bottom are:

$$(q^2(\eta), q^2 l(\eta)) = (B_1^{2/3} u_\tau^2(0), 0) \tag{19}$$

$$(q^2(-H), q^2 l(-H)) = (B_1^{2/3} u_\tau^2(-H), 0), \; (Q^2(-H), Q^2 l(-H)) = (B_1^{2/3} u_\tau^2(-H), 0) \tag{20}$$

where $u_I(0)$ and $u_I(-H)$ are friction velocities.

Lateral boundary conditions are given at solid and open boundaries (see Figure 3). At the solid boundaries the non-slip conditions are used. At the open boundary a new boundary condition is used. It is a based-Newtonian relaxation technique for sea level. The computational domain is a closed area that is divided into an internal zone and relaxation zones along the open boundaries. The boundary conditions at the outer boundary of relaxation zones are non-slip conditions. The equation for surface elevation was derived by the integration of continuity equation (4) from bottom to surface. The modified equation is:

$$\frac{\partial \eta}{\partial t} + \frac{\partial \overline{u}(H+\eta)}{\partial x} + \frac{\partial \overline{v}(H+\eta)}{\partial y} = -\frac{\eta - \eta_B}{T}\alpha \tag{21}$$

The right side is Newtonian relaxation term, where α is relaxation parameter, that is $\alpha = 1$ in the relaxation zone and $\alpha = 0$ outside of it, η_B is prescribed elevation on the boundary and T is relaxation time. The relaxation time is a parameter chosen to satisfy non-reflecting condition for disturbances coming into the relaxation zone.

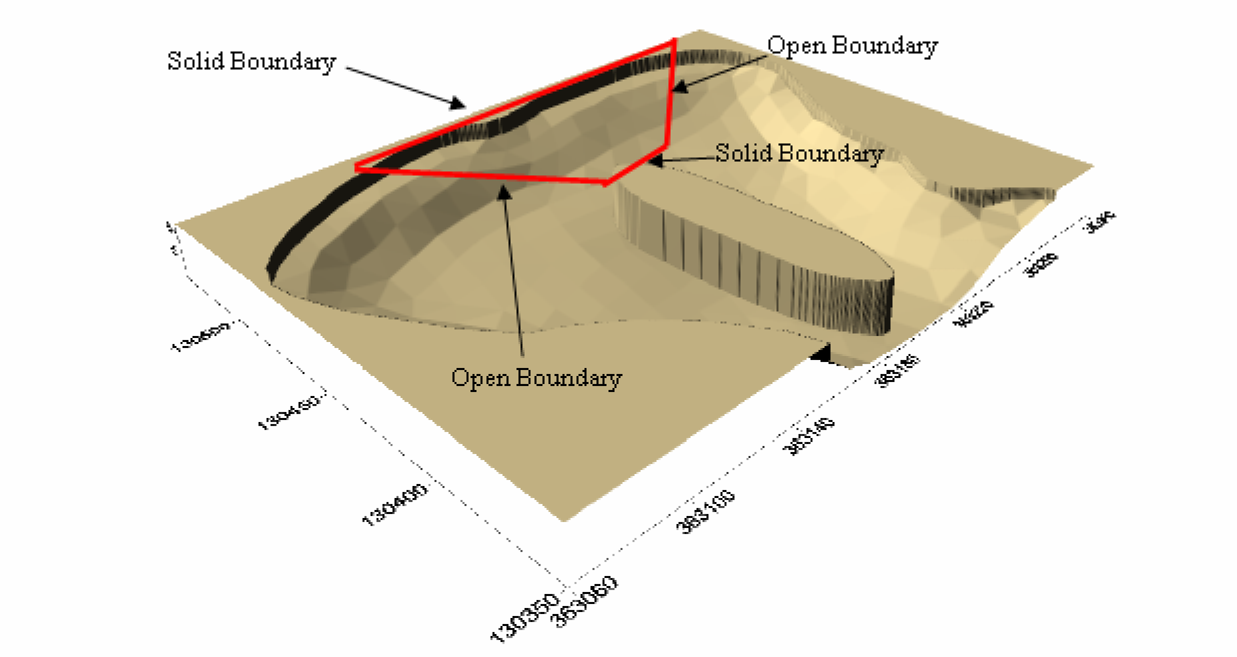

Figure 3. Example computational area with various boundary types.

Model Validation with Lab Data

The model was validated using laboratory data from the free-propeller experiments of Schokking (2002). The experiments were carried out in a laboratory tank (2.0 x 1.9 x 0.48 m^3) at Delft University of Technology. A propeller was installed in deeper water on the opposite side from an inclined slope. Propeller velocities were measured at approximately 100 locations within the velocity field, providing an extensive and reliable data set for validation of the VH-PU model. Figure 4 shows the laboratory measurement setup, including the locations of the velocity measurement points and the stationary propeller.

The numerical model domain size was 80x30x40 cells with the propeller jet simulated as a square jet with equivalent flow area (10.8 x 6.6 cm^2) and constant velocity U_0 = 1.38 m/s, which corresponds to the propeller momentum in the experiment. Figure 5 shows cross-sections of velocity at times 0.95, 2.35 and 9.50 seconds during the simulation.

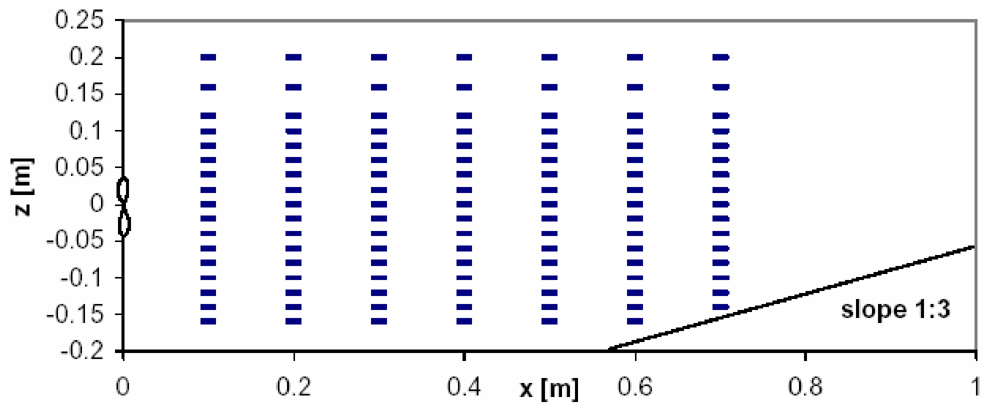

Figure 4. Locations of measurements in laboratory tests (from Schokking 2002)

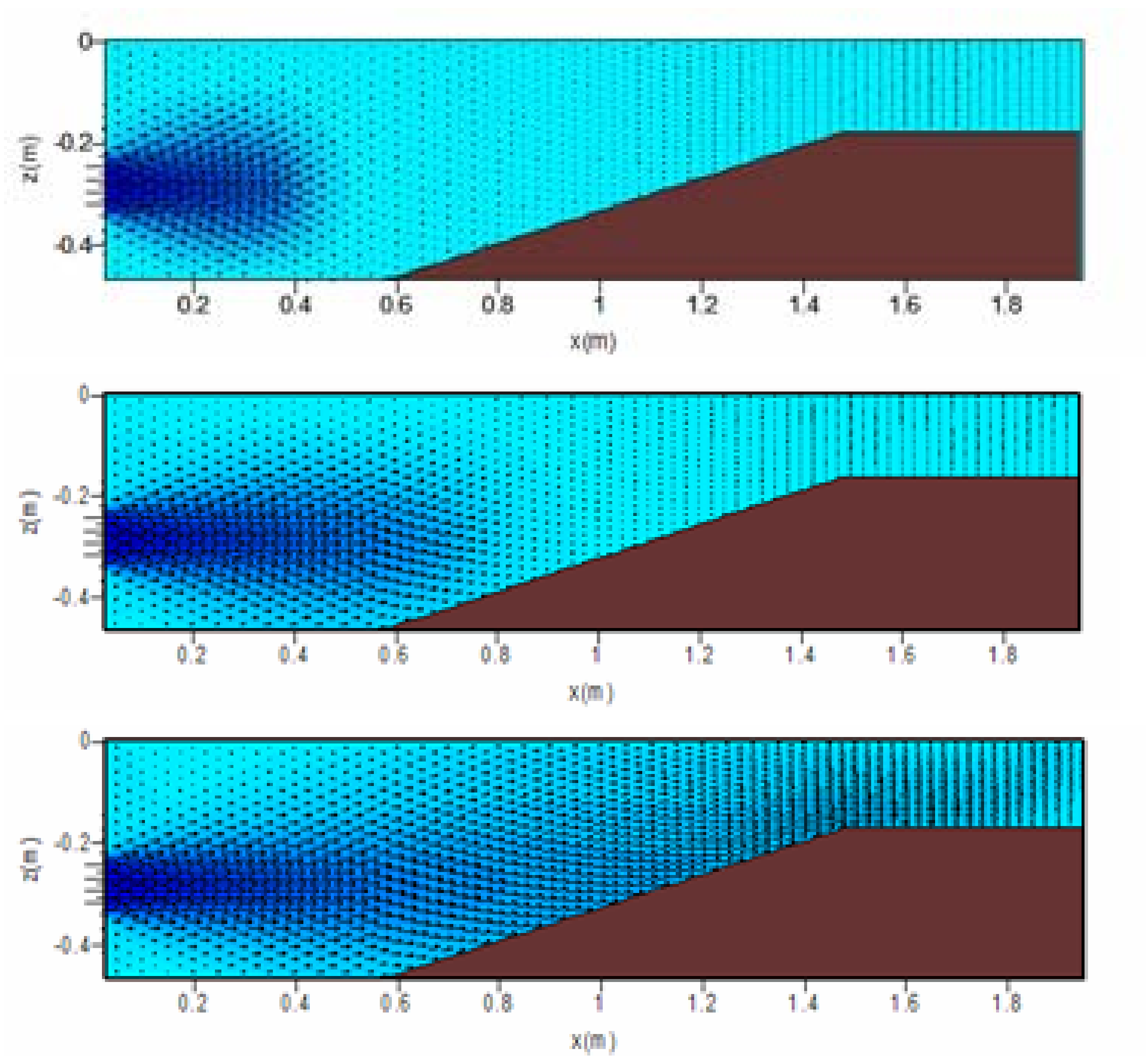

Figure 5. Vertical cross-sections of velocity at time a) 0.95 sec, b) 2.35 sec and c) 9.50 sec

Figure 6 shows a comparison of measured and predicted vertical velocity cross-sections. It is expected that the measured velocities should be smaller than predicted along the propeller axis near the propeller due to the presence of the hub in the laboratory tests and its absence in the numerical model. The results of the simulations were compared with velocities measured in the laboratory from and it was found that the results agree with the measured velocity profiles.

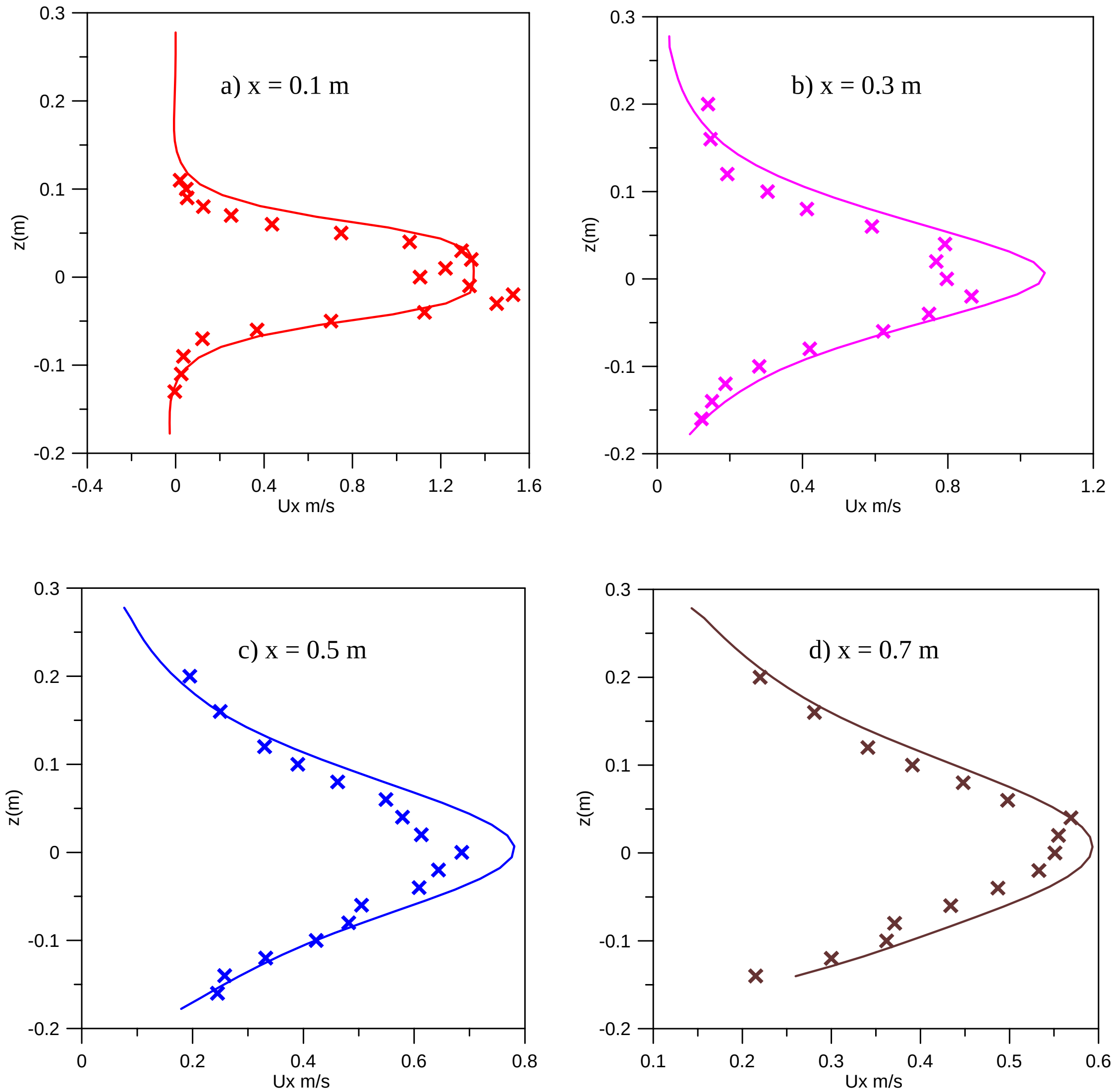

Figure 6. Vertical distributions of mean measured and predicted velocities along the jet axis at varying distance from the propeller. Solid lines are computations; crosses are lab data Schokking (2002).

Model Validation with Field Data

In addition to laboratory data, the VH-PU model was verified using a high-quality set of field measurements. The field data consisted of time series of vertical velocity profiles recorded by an upward-looking Acoustic Doppler Current Profiler (ADCP). Several testing runs were performed using a tug boat, where the tug moved away offshore, after throttling strongly towards the ADCP. The tug position, RPM, thrust and other relevant parameters were recorded at 5-second intervals during the test. Figure 7 shows a schematic of the testing layout. Table 1 presents the tug boat testing parameters that were used during the test and were reproduced using the VH-PU numerical model.

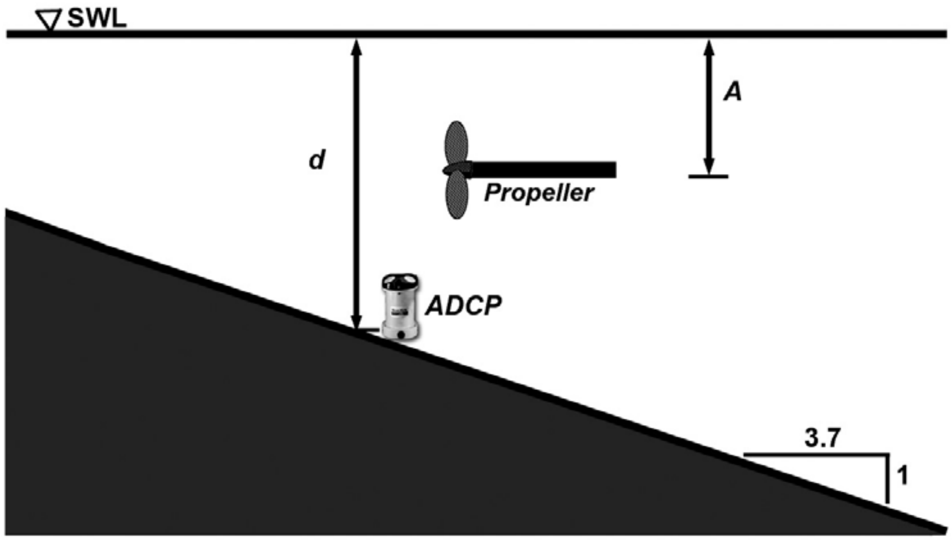

Figure 7. Schematic of field experiment.

Table 1. Field experiment conditions used as input for numerical model.

Test	Propeller Rotation Rate (rps)	Propeller Diameter (m)	K_{tp}	Thrust (N)	Initial Velocity (m/s)	Depth (m)	Distance from Surface to Propeller Axis (m)
1	3.33	1.83	0.16	41,553	3.94	10.4	3.05
2	3.33	1.83	0.29	73,886	5.25	10.3	3.05

Figure 8 shows example cross-sections of horizontal velocity for Test 2. It is clear from the modeling results that the propeller wash is affected by its proximity to the surface. Figures 9 and 10 show vertical current speed profiles recorded by the ADCP (reported as 2-second averages) compared with vertical velocity profiles obtained using the VH-PU model at time steps up to approximately 10 seconds. The vertical profiles extracted from the numerical model take into account the boat displacement. The field experiment showed that the vessel displacement at times greater than 10 seconds into each testing run was too much and that no significant velocities were measured at the ADCP.

The VH-PU model shows good agreement with measured field data during the test. It is argued that stronger controls during testing, most notably better control over vessel positioning and heading, would improve the comparison between measured and predicted velocities. Overall, the results of verification with laboratory tests and full-scale field tests show that the VH-PU predicts propeller/jet wash velocities in a reasonable manner and confirm the practical applicability of the model.

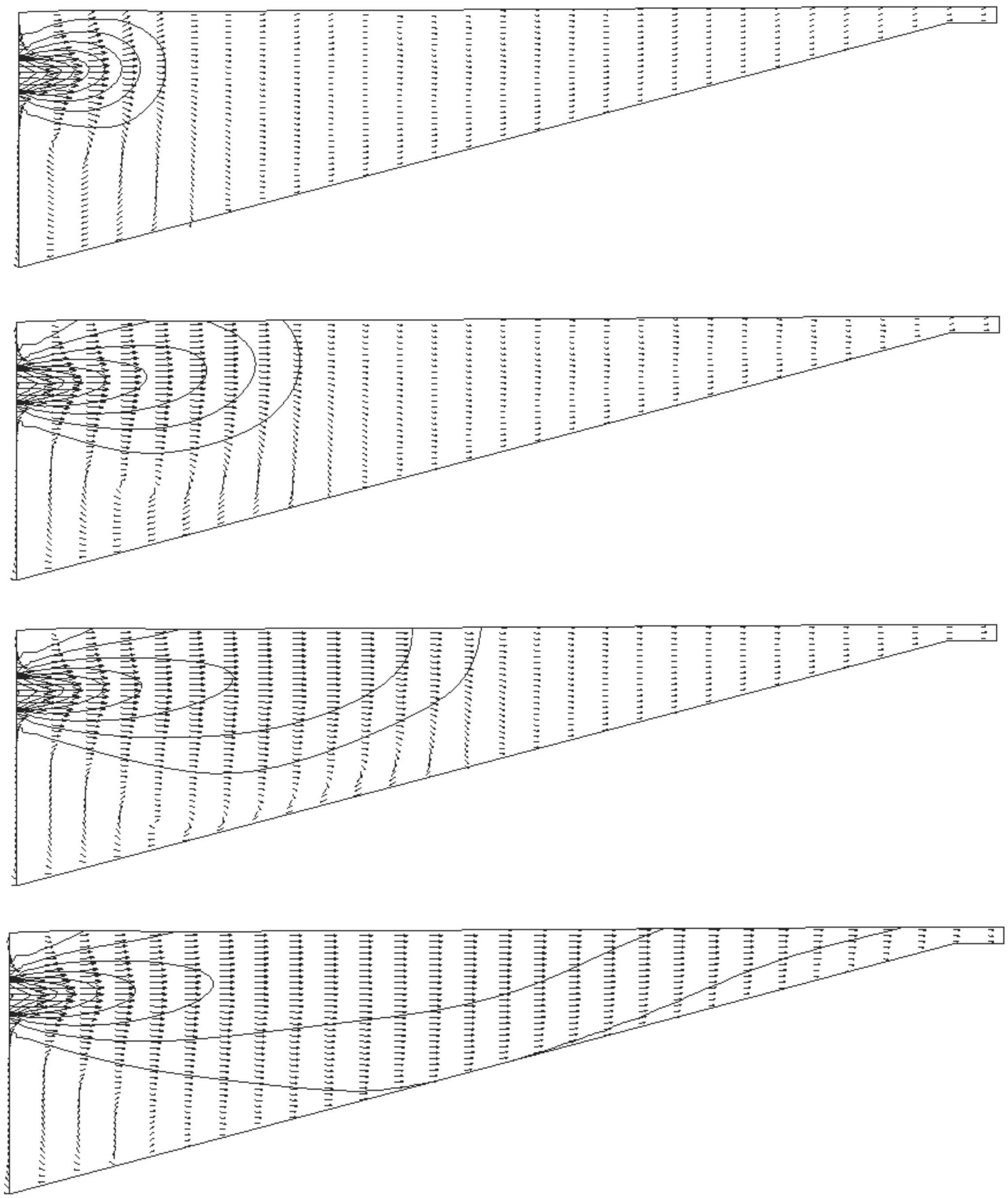

Figure 8. Vertical cross-sections of velocity at the propeller axis for test 2 and time a) 5 sec, b) 15 sec, c) 30 sec and d) 80 sec. Maximum jet velocity is 5.0 m/s with contours at 0.5 m/s intervals.

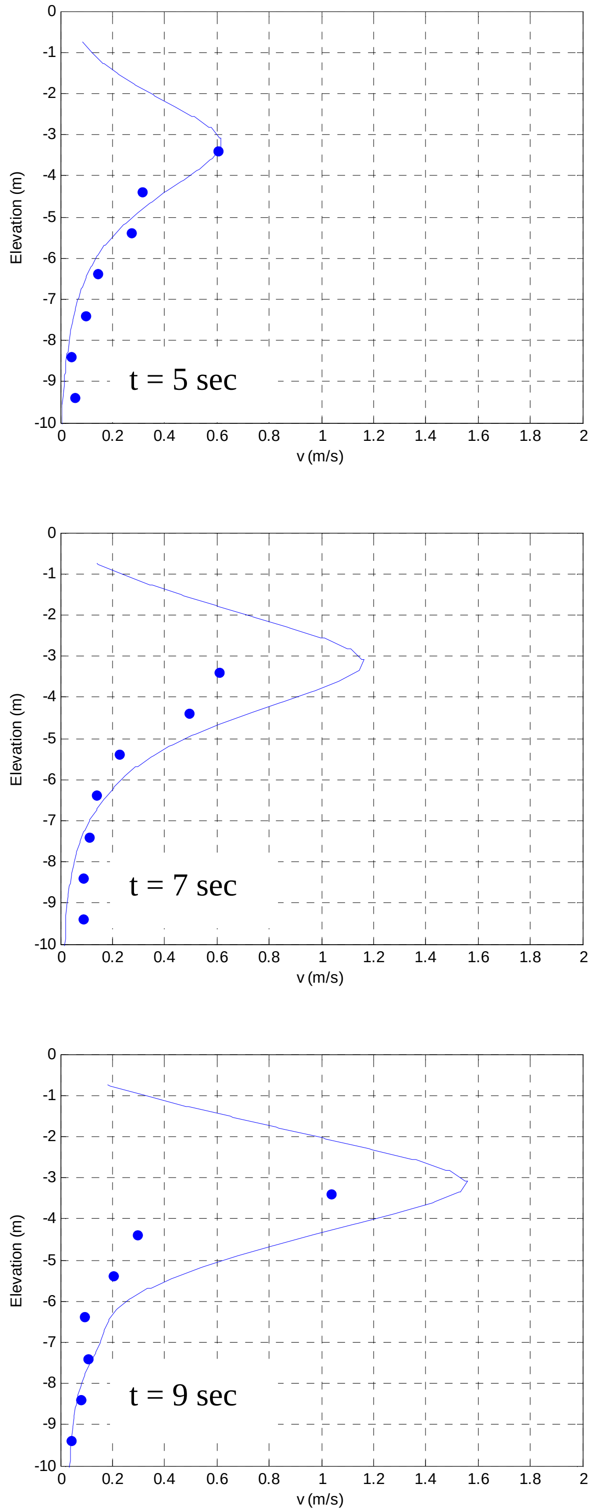

Figure 9. Comparisons of measured and predicted velocities in the vertical cross-section at the propeller axis for test 1. Solid lines are computations, dots are field data.

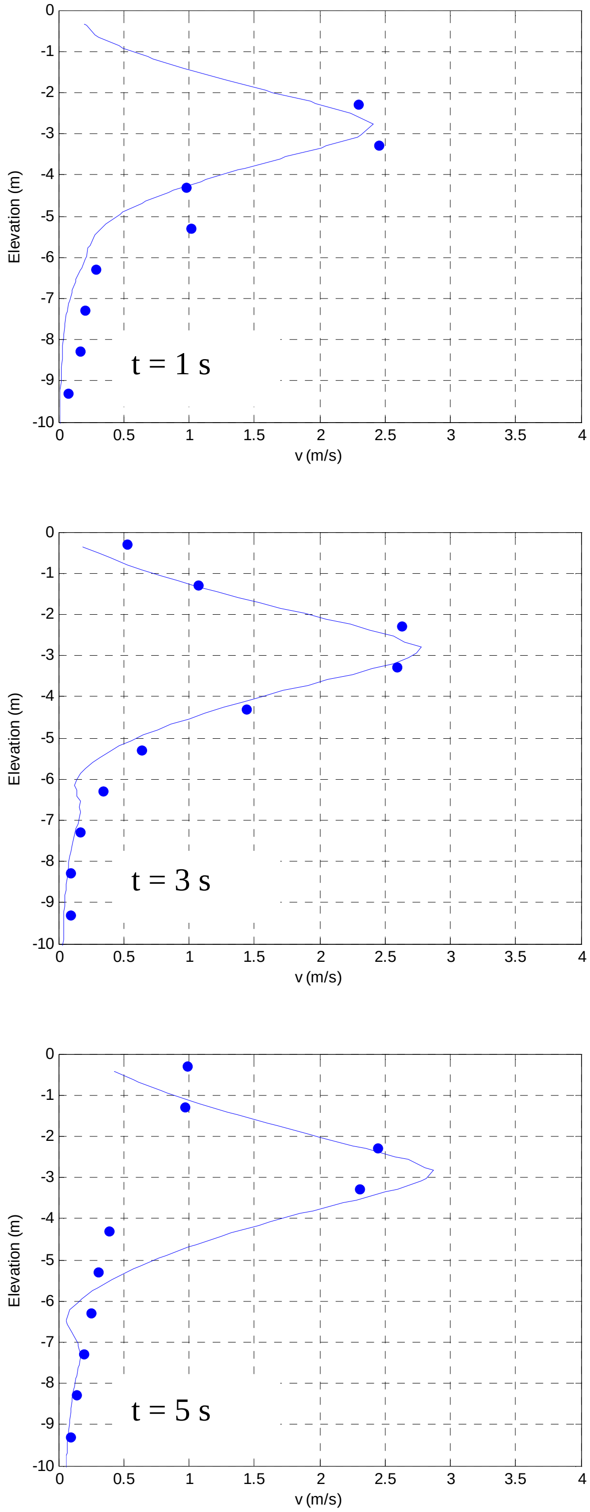

Figure 10. Comparisons of measured and predicted velocities in the vertical cross-section at the propeller axis for test 2. Solid lines are computations, dots are field data.

UNSTEADY PROPWASH MODELING APPLICATIONS

The VH-PU model has been applied successfully on several recent projects, including the Mukilteo Multimodal Ferry Terminal Project located in Mukilteo, WA; Keystone Harbor Ferry Terminal Improvement Project located in Keystone, WA; and Lockheed Capping Project located at the Duwamish Waterway, WA. The Lockheed Capping Project challenge was to develop a cap that could withstand the site's exposure to various scouring factors, including wind-waves, vessel wakes, and propwash. Numerical modeling with the VH-PU model determined that hydrodynamic forces from the propellers of maneuvering tug boats should be the project design criteria. The cap was designed with gravel and cobble material of variable thickness. The project was constructed between December 2004 and January 2005. Figure 11 shows an oblique aerial photo of the constructed capping project. Project monitoring has shown that the recommended cap size, thickness, and slope were sufficient to maintain the cap integrity.

Figure 11. Constructed Lockheed capping project oblique aerial photo.

CONCLUSIONS

Next generation numerical modeling tools have recently been developed as part of a federal grant from the CRDF. The advanced propeller/jet wash modeling tool, VH-PU has been validated with high-quality laboratory data and full-scale field measurements and was shown to give good results. The model has been effectively and efficiently used for evaluation of project feasibility, design criteria and environmental impacts on projects in Washington, Texas, Louisiana and California.

REFERENCES

Albertson , M.L., Y.B. Dai, R.A. Jensen, and Hunter Rouse. 1948. *Diffusion of Submerged Jets*. Proceedings of the American Society of Civil Engineers, Paper No. 2409. P. 639-697.

Blaauw, H.G. and E.J. van de Kaa. 1978. *Erosion of Bottom and Sloping Banks Caused by the Screw-Race of Maneuvering Ships*. International Harbour Congress. Antwerp, Belgium.

Blumberg, A.F. and G.L. Mellor. 1987. A description of a three-dimensional coastal ocean circulation model. *Three-Dimensional Coastal Ocean Models*, N. Heaps (ed), Am. Geoph. Union.

Fuehrer, M., Pohl, H. and K. Roemisch. 1987. *Propeller jet erosion and stability criteria for bottom protections of various constructions*. Bulletin of the P.I.A.N.C. No. 58. P.45-56.

Kanarska Y. and V. Maderich. 2003. A *non-hydrostatic numerical model for calculating free-surface stratified flows.* Ocean Dynamics, 53, P. 176-185.

Maynord, Steven. 2000. *Physical Forces near Commercial Tows. Interim Report for the Upper Mississippi Rive – Illinois Waterway System Navigation Study*. U.S. Army Corps of Engineers ENV Report 19.

Mellor, G.L. and T. Yamada. 1982. *Development of a turbulence closure model for geophysical fluid problems.* Reviews of geophysics and space physics, 20, N 4, P. 851-875.

Schokking, L. 2002. *Bowthruster-induced Damage. MS Thesis*, TUDelft P. 143.

Shepsis, V. and D. Simpson. 2000. *Propwash Modeling for CAD Design*, Contaminated Sediment Conference, Massachusetts Institute of Technology (MIT), Boston, 2000.

Verhey, H.J. 1983. *The stability of bottom and banks subjected to the velocities in the propeller jet behind ships.* In Proceedings of the 8th International Harbour Congress. Antwerp, Belgium. June 13–17.